HHS Public Access

Author manuscript

Life Sci. Author manuscript; available in PMC 2020 March 15.

Published in final edited form as:

Life Sci. 2019 March 15; 221: 212–223. doi:10.1016/j.lfs.2019.01.040.

Metabolomic Analysis of Serum and Myocardium in Compensated Heart Failure After Myocardial Infarction

M. Dan McKirnan[1,2], **Yasuhiro Ichikawa**[1], **Zheng Zhang**[1], **Alice E. Zemljic-Harpf**[1], **Sili Fan**[3], **Dinesh Kumar Barupal**[3], **Hemal H. Patel**[1], **H. Kirk Hammond**[2], and **David M. Roth**[1]

[1]Department of Anesthesiology, University of California, San Diego, La Jolla, California, and the Veterans Affairs San Diego Healthcare System

[2]Department of Medicine, University of California, San Diego, La Jolla, California, and the Veterans Affairs San Diego Healthcare System

[3]UC Davis Genome Center, University of California, Davis, California

Abstract

Aims: To determine the metabolic adaptations to compensated heart failure using a reproducible model of myocardial infarction and an unbiased metabolic screen. To address the limitations in sample availability and model variability observed in preclinical and clinical metabolic investigations of heart failure.

Main Methods: Metabolomic analysis was performed on serum and myocardial tissue from rabbits after myocardial infarction (MI) was induced by cryo-injury of the left ventricular free wall. Rabbits followed for 12 weeks after MI exhibited left ventricular dilation and depressed systolic function as determined by echocardiography. Serum and tissue from the viable left ventricular free wall, interventricular septum and right ventricle were analyzed using a gas chromatography time of flight mass spectrometry-based untargeted metabolomics assay for primary metabolites.

Key Findings: Unique results included: a two- three-fold increase in taurine levels in all three ventricular regions of MI rabbits and similarly, the three regions had increased inosine levels compared to sham controls. Reduced myocardial levels of myo-inositol in the myocardium of MI animals point to altered phospholipid metabolism and membrane receptor function in heart failure. Metabolite profiles also provide evidence for responses to oxidative stress and an impairment in TCA cycle energy production in the failing heart.

Corresponding Author: David M. Roth droth@ucsd.edu 858 552-8585 ext. 1091.

Compliance with ethical standards

The manuscript does not contain clinical studies or patient data.

Conflict of interest

DMR and HHP are scientific founders of CavoGene LifeSciences LLC and hold equity interest in the company. HKH is a scientific founder and non-paid consultant of Renova Therapeutics.

CavoGene LifeSciences LLC and Renova Therapeutics were not involved with experimental design, analysis, discussions or in the writing of the manuscript. All other authors have reported that they have no relationships relevant to the contents of this paper to disclose. DMR and HHP are scientific founders of Cavogene. HKH is a scientific founder of Renova Therapeutics. All other authors have reported that they have no relationships relevant to the contents of this paper to disclose.

Significance: Our results revealed metabolic changes during compensated cardiac dysfunction and suggest potential targets for altering the progression of heart failure.

Keywords

Metabolomics; Myocardial infarction; Heart Failure; Taurine; Inosine; Myo-inositol; BCAA

Introduction

Heart failure is a leading cause of morbidity and mortality worldwide [79]. Clinically, multiple factors can influence the severity and progression of heart failure as well as the outcomes following hospitalization [41]. Modeling of heart failure progression in animal models can limit confounding variables (environment, comorbidities, medications) and provide insights into pathogenesis and therapy [3]. Coronary artery disease and subsequent myocardial ischemic injury is a major cause of progression to heart failure [25]. Coronary ligation models of myocardial ischemic injury are limited by variable coronary anatomy and subsequent variable infarct size and location that reduce the power of such studies. Cryoablation effectively yields reproducible areas of myocardial infarction (size, depth, and location) for more precise study of compensated cardiac dysfunction [44]. Although cryo-injury does not replicate the clinical MI, it does provide a model to study myocardial metabolism after the heart has adapted to a fixed injury.

Metabolic dysfunction (dysregulation) is an important component of the complex pathogenesis of heart failure [14, 46, 51, 67, 78]. High energy consumption and metabolic flexibility for substrate utilization challenges our understanding of impaired energy production in the failing heart [46, 51, 78]. Metabolomics is the study of chemical compounds involved in metabolic and biochemical pathways of carbohydrate, fatty acid, amino acid, ketone, nucleoside, phospholipid and polyamine metabolism [32, 48, 62]. Metabolomic analyses are important in cardiovascular medicine [17], but patient studies are often limited to analysis of blood and urine since patient tissue samples are not readily attainable and heterogeneous due to age differences, comorbidities, different drug treatments, and nutritional habits [32, 48, 62].

We have designed the current investigation to address limitations of experimental model design, confounding variables of clinical metabolomics studies and tissue availability for metabolomics in a model of left ventricular free wall cryoablation and chronic myocardial dysfunction. For the first time a non-targeted, unbiased metabolic profiling of serum and regional left and right ventricular tissue was performed in the rabbit cryoablation model. We show that cryoablation of the left ventricular free wall produces a reproducible region of myocardial infarction and reduced ejection fraction that is maintained for 12 weeks. These stable changes in left ventricular function prior to overt heart failure are accompanied by alterations in serum and myocardial metabolism that differ among right ventricle (RV), intraventricular septum (IVS) and non-infarcted left ventricular free wall (LVFW). The results provide important information regarding the metabolic changes involved in chronic cardiac dysfunction and the progression of heart failure.

Materials and methods

New Zealand White Rabbits (NZW) were purchased from Western Oregon Rabbit Co., Philomath, OR. All procedures were conducted in accordance with NIH guidelines, the *Guide for the Care and Use of Laboratory Animals* (National Academy of Science) and approved by the Institutional Animal Care and Use Committee at the VA San Diego Health Care System. Male and female NZW rabbits (n= 10) weighing 2.8 to 3.2 kg underwent a sterile left thoracotomy wherein a cryoprobe (Brymill Model #205–1) was used to induce a myocardial infarction by freezing a section of the left ventricular free wall (Fig. 1) [44]. Surgery was induced with ketamine (25–50 mg/kg) + midazolam (1–2 mg/kg) IM followed by 1–3 % isoflurane via face mask. Rabbits were then intubated, ventilated and maintained on 1–3% isoflurane. A thoracotomy was then performed between the 3rd and 4th ribs and the pericardium was opened to provide access to the left ventricle free wall. A 3–0 silk suture was introduced through the apex of the heart to provide control of the heart during freezing. (see Fig 1) The 1 cm cryoprobe cooled with liquid N2 was placed on the anterio-lateral ventricular free wall midway between the apex and base of the heart to induce the MI. Probe pressure was applied such that the myocardial tissue (2–4 mm) around the probe blanched. The probe was applied for a total of 3 minutes to achieve a transmural infarct as previously described [5]. Fluid support and cardiovascular drugs were used to restore normal hemodynamics prior to closing the chest and recovering the animal. A thoracotomy and pericardectomy alone was performed on a group of six NZW rabbits (3 males & 3 females) of similar size to provide sham controls for the 12- week study. At necropsy, hearts were arrested in diastole and infarct size was assessed immediately post-mortem. The endocardial area of the left ventricular free wall plus septum was traced on plexiglass at a fixed wall thickness. The scar was excised from the LV and the area traced and measured by planimetry using Image J - NIH (https://imagej.nih.gov/ij/). Infarct size was calculated by the ratio of scar area and total LV endocardial area.

Echocardiography

Left ventricular function was assessed during the time course of the study using echocardiography with a Philips SONOS 5500 unit and a S12 probe (frequency: 5–12 MHz) (Philips, Amsterdam, Netherlands). Rabbits were sedated with midazolam (2 mg/kg, intramuscular) and 1.5% isoflurane was administered via inhalation. Guided M-mode imaging was performed at the left ventricular papillary muscle level, and fractional shortening (FS) was calculated from LV dimensions at end-systole (ESD) and end-diastole (EDD) as FS = (EDD-ESD)*100/EDD. LV ejection fraction (EF) was calculated using the Teichholz method [72]. Velocity of circumferential fiber shortening (Vcf) was calculated from EDD, ESD and ejection time (ET) as Vcf=(EDD-ESD)/(EDD*ET).

Serum and Tissue Collection

Blood and tissue were obtained after completion of the 12-week echocardiography study. All animals were anesthetized with isoflurane via a nose cone. Deep anesthesia was achieved with 4–5% isoflurane and the chest was opened by a midline incision and sternal split. Methods for tissue collection were consistent with the report that less variability is obtained when tissue is obtained under anesthesia rather than post-euthanasia [52]. The heart was

exposed and venous blood obtained by needle puncture of the right ventricle. Animals then were heparinized (500 IU heparin/kg body weight) and KCl (16 mEq/L) was injected through the apex of the left ventricle until the heart arrested in diastole. The heart was immediately removed and placed in a slurry of ice-cold saline. Blood was flushed from the heart by retrograde perfusion of the coronary arteries via a short section of the proximal aorta. The heart was maintained in the cold saline slurry during sectioning. Myocardial sections of the heart regions were placed in cryotubes and flash frozen in liquid nitrogen. Serum and tissue samples were maintained in a −80° C freezer until shipment on dry ice to the West Coast Metabolomics Center at the University of California Davis for metabolomic analysis. Serum was prepared as follows: Blood was placed in red top tubes and allowed to stand at room temp for 30 minutes. Tubes were then placed in a refrigerated centrifuge (4°C) and spun at 2000 rcf for 15 minutes. The supernatant was transferred to a cryotube and then flash frozen in liquid nitrogen.

Metabolomic Sample Preparation

Metabolites were extracted from a 20 μL serum aliquot using 1 ml of degassed and cold (at −20°C) acetonitrile:isopropanol:water (3:3:2, v/v/v) mixture. For the heart samples, 6 mg of frozen tissue was homogenized using a GenoGrinder 2010 (SPEX SamplePrep) for 2 min at 1350 rpm. Samples were vortexed for 10 seconds, shaken for 5 minutes and then centrifuged for 2 minutes at 14,000 rcf. Dried samples were cleaned with 0.5 mL of an acetonitrile:water (1:1, v/v) mixture, decanted and evaporated. Two 450 μL supernatant aliquots was transferred to new tubes. One tube was stored as a backup aliquot and another was dried using CentrVap. For derivatization, a 10 μL of methoxyamine hydrochloride in pyridine (40 mg/mL) was added to each sample and then shaken at 30°C for 90 min. Then 90 μL of *N*-methyl-*N*-(trimethylsilyl) trifluoroacetamide (MSTFA, Sigma-Aldrich) was added for trimethylsilylation. C8–C30 fatty acid methyl esters (FAMEs) were added as internal standard for retention time correction. Then samples were shaken for 30 minutes at 37°C. These derivatized samples were analyzed by GCMS. GC/MS was chosen for this study because it can reliably measure primary metabolites from central metabolic pathways that were dysregulated in cells under a stress [8, 22]. Furthermore, the West Coast Metabolomics Center uses BinBase [68], a fully automated GC/MS data processing software to generate data matrix with minimum false positive peaks.

Injector conditions

An Agilent 6890 gas chromatography instrument equipped with a Gerstel automatic linear exchange systems (ALEX) which included a multipurpose sample dual rail and a Gerstel cold injection system. The temperature program for the injection system was: 50°C to 275°C final temperature at a rate of 12 °C/s and hold for 3 minutes. Injection volume was 0.5 with 10 μL/s injection speed. Injection mode was splitless with a purge time of 25 seconds. The injector liner was changed after every 10 samples. The injection syringe was washed with 10 μL of ethyl acetate before and after each run.

Gas chromatography conditions

A Rtx-5Sil MS column (30 m length, 0.25 mm id, 0.25 μM 95% dimethyl 5% diphenyl polysiloxane film). An additional 10 m long integrated guard column was used. Mobile

phase was 99.9999% pure helium gas with a flow rate of 1ml/min. The gas chromatography temperature program was: held at 50°C for 1 min, ramped at 20°C/min to 330°C and then hold for 5 min.

Mass spectrometer settings

A Leco Pegasus IV time of flight mass spectrometer was used for acquiring the mass spectral data. The spectrometer was operated using the Leco ChromaTOF software vs. 2.32 (St. Joseph, MI). The transfer line temperature between gas chromatograph and mass spectrometer was set to 280°C. Electron impact ionization at 70V was employed with an ion source temperature of 250°C. Acquisition rate was 17 spectra/second, with a scan mass range of 85–500 Da.

Data Processing

Raw data files were preprocessed directly after data acquisition and stored as ChromaTOF-specific *.peg files, as generic *.txt result files and additionally as generic ANDI MS *.cdf files. ChromaTOF vs. 2.32 is used for data preprocessing without smoothing, 3 s peak width, baseline subtraction just above the noise level, and automatic mass spectral deconvolution and peak detection at signal/noise levels of 5:1 throughout the chromatogram. Apex masses were reported for use in the BinBase algorithm. Result *.txt files were exported to a data server with absolute spectra intensities and further processed by a filtering algorithm implemented in the metabolomics BinBase database. The BinBase algorithm (rtx5) used the settings: validity of chromatogram (10^7 counts s-1), unbiased retention index marker detection (MS similarity>800, validity of intensity range for high m/z marker ions), retention index calculation by 5th order polynomial regression. Spectra were cut to 5% base peak abundance and matched to database entries from most to least abundant spectra using the following matching filters: retention index window ±2,000 units (equivalent to about ±2 s retention time), validation of unique ions and apex masses (unique ion must be included in apexing masses and present at >3% of base peak abundance), mass spectrum similarity must fit criteria dependent on peak purity and signal/noise ratios and a final isomer filter. Failed spectra were automatically entered as new database entries if s/n >25, purity 80%. All thresholds reflect settings for ChromaTOF v. 4.0. Quantification was reported as peak height using the unique ion as default, unless a different quantification ion is manually set in the BinBase administration software BinView. A quantification report table was produced for all database entries that were positively detected in more than 10% of the samples of a study design class (as defined in the miniX database) for unidentified metabolites. A subsequent post-processing module was employed to automatically replace missing values from the *.cdf files. Replaced values were labeled as ‘low confidence’ by color coding, and for each metabolite, the number of high-confidence peak detections is recorded as well as the ratio of the average height of replaced values to high-confidence peak detections. These ratios and numbers were used for manual curation of automatic report data sets to data sets released for submission.

Statistical Analysis, and Metabolic network mapping

Data were normalized to the total sum of known compounds in each sample and then log2 transformed. Welch’s t-test was used to identify significantly different compounds in MI

group in comparison to the Sham group. Metabolites were mapped into a metabolic network graph using the MetaMapp software [7] and visualized using the Cytoscape software.

Results

Cryo-injury MI model characteristics

Infarct size was 29 ± 3 % of the left ventricle including septum. Heart size was greater in the MI than the sham animals as reflected in the ratios of heart weight/body weight and LV weight/body weight (Table 1). This was confirmed by echocardiography which revealed a 32% greater end diastolic dimension in MI compared to sham rabbits (Table 2, Suppl Fig. 6). Systolic function, as reflected in ejection fraction, was reduced below sham values at 4 weeks post MI (38 vs 57 %) and remained at this level through the 12-week follow-up period (35 vs 59 %).

Serum metabolites

Normalized peak intensity levels for metabolites in serum are listed in Table 3 and depicted by volcano plot (Fig. 2a) and network regions (Fig. 2b and c). Phosphate and malic acid, were reduced by 40% in MI rabbits compared to shams (Table 3 and Fig. 2). Slight elevations in the lipids, palmitic and stearic acid, were noted for MI rabbits, but only the stearic acid signal was significant. Products of ascorbic acid metabolism, dehydroascorbic acid and threonic acid, were both elevated in the serum of MI rabbits. The amino acid β-alanine was decreased by 40% in MI animals, but branched-chained amino acids, valine, leucine and isoleucine, were not different between groups. Myo-inositol levels in MI rabbits were 50% higher than shams, but this did not achieve statistical significance ($p = 0.07$).

Myocardial metabolites

A VENN diagram shows the numbers for significantly different metabolites between MI and Sham rabbits in the three myocardial regions (Fig. 3). Levels for individual metabolites are listed in Table 3 and Suppl Table 1 and depicted by volcano plots (Fig. 4) and network regions (Fig. 5). Myocardial tissue from MI rabbits revealed marked increases in the levels of the metabolites inosine and taurine compared to shams. The left ventricular free wall (LVFW), interventricular septum (IVS) and right ventricle (RV) exhibited this response. The increase in inosine levels ranged from 1.4 to 1.7 fold in the three regions while the taurine level increase ranged from 1.9 fold for the IVS to 3.5 fold for the LVFW. Hypoxanthine, a degradation product of inosine was increased in a similar manner in the RV alone. The marginal reductions in phosphate for the LVFW and RV of MI rabbits were not significant. Organic acids and TCA cycle intermediates reduced by MI included 2-hydroxyvaleric acid and succinic acid which were lower in both the IVS and RV. The elevated dehydroascorbic acid levels in the IVS and threonic acid levels in the RV compared to shams was consistent with the response observed for serum. Excluding taurine, the levels for aromatic and amino acid compounds varied across the three chambers. The LVFW tissue from MI animals had reduced levels for aminomalonate and increased phenylalanine levels compared to shams. IVS tissue from MI animals showed increased levels for phenylalanine (50%) and glutathione (70%), but decreased levels for beta alanine (40%), benzoic acid (20%) and nicotinamide (30%) compared to shams. Comparable reductions in beta alanine levels was

noted for both serum and IVS of the MI rabbits. Noradrenaline signal was lower in the LVFW region of MI animals, but this difference failed to reach statistical significance ($p = 0.055$). An increase in methionine levels was observed in the RV tissue of MI rabbits. Reductions in myo-inositol levels were noted for all three myocardial regions but only the decrease in the LVFW was statistically significant. Lipid metabolites, glycerol and palmitoleic acid, levels were reduced in the IVS of MI animals, while linolenic acid levels were increased in the LVFW region. MI altered the urea cycle as hydroxycarbamate NIST levels in the IVS and urea levels in the LVFW were decreased compared to shams. Sulfate levels were increased by two-fold in the LVFW of MI animals.

DISCUSSION

Metabolomics has been studied in multiple cardiovascular diseases to identify target metabolites that could provide insights into mechanisms of dysregulation, severity of disease, disease progression, and potential targets for treatment [6, 17, 48]. The goal of the current study was to address limitations of model/patient variability and tissue and serum availability present in previous pre-clinical and clinical metabolomic studies. The cryo-myocardial infarction model in our hands produced a reproducible myocardial infarction (MI), of 30 % of the LV free wall, with echocardiographic findings comparable to previous coronary occlusion MI models in the rabbit [77]. Clinical studies using metabolomic platforms to study heart failure have relied primarily on blood analysis, however limited urine collection and tissue sampling studies have been reported [9, 20, 28, 32, 40]. Extensive discussions of this topic can be found in recent reviews [6, 17, 32, 48]. Spectrograph signals for serum and tissue analytes revealed that a reproducible myocardial infarction produced significant alterations in myocardial metabolites.

Increases in taurine were seen in all three regions of the heart examined. Taurine is a ubiquitous amino sulfonic acid with diverse biological functions found in high concentrations in heart and muscle [58]. Taurine plays a role in Ca++ homeostasis and contractile function [54, 56], improves energy metabolism [59], and indirectly regulates oxidative stress via mitochondrial complex I and the endoplasmic reticulum [36, 38]. Taurine also plays a role in membrane stabilization through direct interactions with phospholipids [57] and serves as a modulator of protein kinases and phosphatases [34]. Taurine deficiency is associated with diminished autophagy [39] and decreased levels of the transcription factor PPARaα [25] a key regulator of fatty acid metabolism. Taurine supplementation after experimental MI decreased apoptosis, oxidative stress, metalloproteinase activation (MMP-2 & 9) and improved cardiac energy metabolism [4]. Taurine has been studied as a potential therapeutic for heart failure with a focus on its antagonism of neurohumoral factors [5, 35, 56]. In a small randomized, double-blind study in heart failure patients, taurine supplementation improved ECG parameters, exercise capacity, and hemodynamic responses to exercise [2]. Plasma taurine levels are elevated in patients with advanced heart failure [16, 49], but serum taurine was not elevated in our MI rabbits with compensated heart failure. However, our findings are consistent with reports that taurine content is increased in hearts of heart failure patients and experimental models of heart failure [33, 50, 53, 71]. The increased levels of taurine in hearts of our rabbits may be linked to a reduction in β-alanine in both the serum and the IVS given that β-alanine is a

nonessential amino acid that blocks taurine transport [37, 58]. Further investigations are warranted for potential mechanism, relevance, and therapeutic implications of our findings of an increased taurine signal in hearts with stable cardiac dysfunction after MI.

The next largest signal in our study suggests a significant increase in inosine levels in all three heart regions after MI. Inosine is a product of irreversible degradation of adenosine by adenosine deaminase. Inosine can then be converted to hypoxanthine by a phosphorylase. Although unchanged in serum, inosine levels were increased in all regions of our MI rabbit hearts while hypoxanthine was increased in the RV alone (1.5 fold). The fact that adenosine was not altered in serum and tissue of MI rabbits was surprising since patients in heart failure have been shown to have elevated plasma and decreased tissue levels of adenosine [20, 23]. Our findings of increased inosine levels may suggest a metabolic shift towards energy repletion in the face of oxidative stress [26, 69]. Inosine can increase energy production through the hypoxanthine-IMP-AMP pathway or through the anaerobic pentose pathway (ribose1P) [61]. An anti-inflammatory role for inosine has also been reported [11, 30]. Increased myocardial inosine in our MI rabbits contrasts the reports of unchanged or reduced purines in the rat MI model [24, 27] and cardiomyopathic hamster [47]. In the dog model of pacing-induced heart failure, total adenine nucleotides, ATP and creatinine in the heart were reduced [65]. In our MI rabbits, marginal reductions were noted for creatinine ($p=0.07$) in the LVFW and phosphate in the LVFW ($p=0.10$) and RV ($p=0.08$) (Supp table 1). Whether our observations of an increased myocardial inosine levels in MI rabbits is unique to the species or occurs in the setting of compensated cardiac dysfunction is uncertain.

Myo-inositol is a prominent component of membrane-incorporated phosphatidylinositol as well as a participant in its free form, with its isomers or its phosphate derivatives in a multitude of cellular processes including metabolic homeostasis and stress responses [13]. Levels for serum myo-inositol were increased and heart tissue signals were decreased to varying degrees in our MI rabbits. Elevated plasma myo-inositol has been reported in heart failure patients and animal heart failure models [3, 19, 49, 75] and plasma myo-inositol levels were increased in proportion to the severity of heart failure [19]. The increase in serum myo-inositol may reflect an increased synthesis by the kidney to compensate for the reduced tissue concentrations, altered myo-inositol metabolism or an increase release from the tissue. Reduced tissue myo-inositol suggests alterations in lipid metabolism in our rabbit MI model [13]. Reduced energy production in failing hearts in part results from a metabolic shift from mitochondrial oxidative metabolism towards glycolysis with decreased lipid metabolism, particularly free fatty acid oxidation, playing a role in this transition [46, 48]. Signals representative of lipid metabolism in our MI model included reduced glycerol and palmitoleic acid in the IVS, increased linolenic acid in the LVFW and increased stearic acid in serum. Cholesterol was elevated in the RV of our MI rabbits. Taken together these observations suggest altered lipid substrates and metabolism in chronic stable heart failure as well as potential myo-inositol induced changes in signaling and membrane structure.

Our results suggest additional alterations in response to oxidative stress in the face of compensated heart failure [29]. Glutathione (GSH) is an aminothiol that plays an important role in defense of ROS and regenerating other antioxidants, including Vitamin C [45].

Dehydroascorbic acid, the fully oxidized form of vitamin C, is reduced spontaneously by glutathione (GSH), as well as enzymatically in reactions using GSH or NADPH [45]. Ascorbic acid levels were not different in our MI and Sham rabbits, but increased turnover or degradation was evident in our MI animals by the elevated dehydroascorbic acid levels in serum and IVS and the increased threonic acid signal in serum and RV. Both GSH and dehydroascorbic acid levels in the IVS of MI rabbits were 1.8 fold higher than the IVS of shams. Varied responses have been reported for glutathione, antioxidant molecules dehydroascorabic acid and alpha-tocopherol in blood or tissue of heart failure patients and animal models of heart failure that may reflect differences in comorbidities, degrees of heart failure, species differences and model selection [15, 18, 42, 47, 60, 64] In a rabbit model of heart failure, supplements of vitamin C and vitamin E prevented increases in ROS formation and improved LV systolic function [31]. The development of heart failure also may activate the pentose phosphate pathway (PPP) as a defense against oxidative stress by regenerating reduced glutathione (GSH) [48, 74]. Kato et al 2010 [42] reported that the activity of the rate limiting enzyme in the PPP, glucose-6-phoshpate dehydrogenase, increased in the transition from compensated LV hypertrophy to heart failure in the Dahl salt-sensitive rat providing a shunt for glucose oxidation as an alternative to anaerobic glycolysis in heart failure. Additionally, reactive oxygen species arising from the mitochondrial electron chain termed “electron leak” has been linked to Complexes I and III that contain Iron-sulphur clusters [64]. We noted elevated signals for methionine, glutathione, sulfate and taurine in the myocardium of MI rabbits suggesting a role for sulfur containing compounds in the metabolic response to MI induced myocardial dysfunction. These findings warrant further study.

Multiple studies of metabolism in heart failure have examined TCA cycle intermediates including succinic and malic acid and amino acids responsible for the replenishment of TCA intermediates, termed anaplerosis including phenylalanine and tyrosine and branched chain amino acids (BCAAs: valine, leucine and isoleucine). Branched-chained amino acids have been of particular interest as increased blood levels have been linked to cardiovascular disease [12, 63, 70]. However, plasma and tissue TCA intermediates and BCAAs levels have been variable across studies of heart failure in humans and animal models [3, 9, 20, 21, 28, 42, 43, 47, 55, 70, 73, 75, 76, 80]. Our MI rabbits had reduced succinic acid levels in the IVS and RV and reduced serum malic acid, but serum and tissue BCAAs were not different from shams. However, phenylalanine levels were increased in the MI rabbit hearts. This is consistent with rodent models of heart failure reporting elevated tissue levels of phenylalanine [42, 43, 47] as well as tyrosine [43]. Multiple human studies of heart failure have reported elevated plasma phenylalanine and tyrosine [32], while studies of end-stage heart failure found reduced plasma and tissue levels of both amino acids [1, 20]. LVAD therapy did not increase the levels of phenylalanine and tyrosine in plasma [1], but tissue levels were restored to normal [20]. Reduced TCA cycle intermediates in the myocardium in heart failure point to reduced anaplerosis. Further study is needed to determine the role BCAAs and the amino acids phenylalanine and tyrosine play in the dysmetabolism of heart failure.

Limitations:

Myocardial function was reduced but unchanged between 4- and 12-weeks after MI suggesting the metabolic alterations observed reflect a stable compensated state prior to overt heart failure. It is acknowledged that the cryo-injury does not replicate the clinical setting of MI. However, the extent of infarcted myocardium should be the major determinant of metabolic changes at this late stage of compensated heart failure rather than the method of MI induction. Some of the variability in metabolites across the three chambers may be due to chamber dependent metabolic patterns [66]. Furthermore, metabolomic studies cannot determine whether a metabolite is reduced because of decreased production, increased degradation and/or uptake, or both. We also employed an un-biased mass spectrometric analysis that is only capable of detecting spectrographic signals for multiple metabolites. Future work is warranted to verify various compounds and /or pathways of particular interest.

Conclusion

The rabbit model of cryo-myocardial infarction offered a well-controlled and reproducible method to compare both serum and myocardial metabolites in compensated heart failure. Novel findings included signals pointing to increases in taurine and inosine levels and decreased myo-inositol levels in the myocardium of our MI rabbits compared to shams. Our results indicate sulfur containing compounds such as taurine, glutathione, methionine, play a role in the metabolic responses to heart failure. Findings for several metabolites point to an impairment in TCA cycle energy production and a metabolite response to oxidative stress in the failing heart. The results provide new information regarding the metabolic changes involved in compensated cardiac dysfunction and the progression of heart failure.

Supplement Tables 1 & 2[10]

Supplementary Material

Refer to Web version on PubMed Central for supplementary material.

Acknowledgements

Funding: The work was supported by Veteran Affairs Merit Awards from the Department of Veterans Affairs (http://www.sandiego.va.gov) BX000783 (DMR), BX003774 (HKH) and BX001963 (HHP), National Institutes of Health (https://www.nih.gov) HL091071 (HHP), HL107200 (HHP, DMR), HL066941 (HKH, DMR, HHP). The authors are grateful to Matthew O. Spellman and Mehul Dhanani for their excellent technical support.

References

1. Ahmad T, Kelly JP, McGarrah RW, Hellkamp AS, Fiuzat M, Testani JM, Wang TS, Verma A, Samsky MD, Donahue MP, Ilkayeva OR, Bowles DE, Patel CB, Milano CA, Rogers JG, Felker GM, O'Connor CM, Shah SH, Kraus WE (2016) Prognostic Implications of Long-Chain Acylcarnitines in Heart Failure and Reversibility With Mechanical Circulatory Support. J Am Coll Cardiol 67:291–299 doi:10.1016/j.jacc.2015.10.079 [PubMed: 26796394]
2. Ahmadian M, Dabidi Roshan V, Ashourpore E (2017) Taurine Supplementation Improves Functional Capacity, Myocardial Oxygen Consumption, and Electrical Activity in Heart Failure. J Diet Suppl 14:422–432 doi:10.1080/19390211.2016.1267059 [PubMed: 28118062]

3. Alexander D, Lombardi R, Rodriguez G, Mitchell MM, Marian AJ (2011) Metabolomic distinction and insights into the pathogenesis of human primary dilated cardiomyopathy. Eur J Clin Invest 41:527–538 doi:10.1111/j.1365-2362.2010.02441.x [PubMed: 21155767]
4. Ardisson LP, Rafacho BP, Santos PP, Assalin H, Goncalves AF, Azevedo PS, Minicucci MF, Polegato BF, Okoshi K, Marchini JS, Barbisan LF, Fernandes AA, Seiva FR, Paiva SA, Zornoff LA (2013) Taurine attenuates cardiac remodeling after myocardial infarction. Int J Cardiol 168:4925–4926 doi:10.1016/j.ijcard.2013.07.091 [PubMed: 23890888]
5. Azuma J, Sawamura A, Awata N, Ohta H, Hamaguchi T, Harada H, Takihara K, Hasegawa H, Yamagami T, Ishiyama T, et al. (1985) Therapeutic effect of taurine in congestive heart failure: a double-blind crossover trial. Clin Cardiol 8:276–282, [PubMed: 3888464]
6. Barba I, Andres M, Dorado DG (2017) Metabolomics and heart diseases: from basic to clinical approach. Curr Med Chem. 10.2174/0929867324666171006151408 doi: 10.2174/0929867324666171006151408
7. Barupal DK, Haldiya PK, Wohlgemuth G, Kind T, Kothari SL, Pinkerton KE, Fiehn O (2012) MetaMapp: mapping and visualizing metabolomic data by integrating information from biochemical pathways and chemical and mass spectral similarity. BMC Bioinformatics 13:99doi: 10.1186/1471-2105-13-99 [PubMed: 22591066]
8. Barupal DK, Pinkerton KE, Hood C, Kind T, Fiehn O (2016) Environmental Tobacco Smoke Alters Metabolic Systems in Adult Rats. Chem Res Toxicol 29:1818–1827 doi:10.1021/acs.chemrestox.6b00187 [PubMed: 27788581]
9. Bedi KC Jr., Snyder NW, Brandimarto J, Aziz M, Mesaros C, Worth AJ, Wang LL, Javaheri A, Blair IA, Margulies KB, Rame JE (2016) Evidence for Intramyocardial Disruption of Lipid Metabolism and Increased Myocardial Ketone Utilization in Advanced Human Heart Failure. Circulation 133:706–716 doi:10.1161/circulationaha.115.017545 [PubMed: 26819374]
10. Benjamini Y, Hochberg Y (1995) Controlling the False Discovery Rate: A Practical and Powerful Approach to Multiple Testing. Journal of the Royal Statistical Society. Series B (Methodological) 57:289–300, http://www.jstor.org/stable/2346101
11. Benowitz LI, Goldberg DE, Madsen JR, Soni D, Irwin N (1999) Inosine stimulates extensive axon collateral growth in the rat corticospinal tract after injury. Proc Natl Acad Sci U S A 96:13486–13490, [PubMed: 10557347]
12. Bhattacharya S, Granger CB, Craig D, Haynes C, Bain J, Stevens RD, Hauser ER, Newgard CB, Kraus WE, Newby LK, Shah SH (2014) Validation of the association between a branched chain amino acid metabolite profile and extremes of coronary artery disease in patients referred for cardiac catheterization. Atherosclerosis 232:191–196 doi:10.1016/j.atherosclerosis.2013.10.036 [PubMed: 24401236]
13. Bizzarri M, Fuso A, Dinicola S, Cucina A, Bevilacqua A (2016) Pharmacodynamics and pharmacokinetics of inositol(s) in health and disease. Expert Opin Drug Metab Toxicol 12:1181–1196 doi:10.1080/17425255.2016.1206887 [PubMed: 27351907]
14. Brown DA, Perry JB, Allen ME, Sabbah HN, Stauffer BL, Shaikh SR, Cleland JG, Colucci WS, Butler J, Voors AA, Anker SD, Pitt B, Pieske B, Filippatos G, Greene SJ, Gheorghiade M (2017) Expert consensus document: Mitochondrial function as a therapeutic target in heart failure. Nat Rev Cardiol 14:238–250 doi:10.1038/nrcardio.2016.203 [PubMed: 28004807]
15. Campolo J, De Maria R, Caruso R, Accinni R, Turazza F, Parolini M, Roubina E, De Chiara B, Cighetti G, Frigerio M, Vitali E, Parodi O (2007) Blood glutathione as independent marker of lipid peroxidation in heart failure. Int J Cardiol 117:45–50 doi:10.1016/j.ijcard.2006.04.065 [PubMed: 16884794]
16. Cheng ML, Wang CH, Shiao MS, Liu MH, Huang YY, Huang CY, Mao CT, Lin JF, Ho HY, Yang NI (2015) Metabolic disturbances identified in plasma are associated with outcomes in patients with heart failure: diagnostic and prognostic value of metabolomics. J Am Coll Cardiol 65:1509–1520 doi:10.1016/j.jacc.2015.02.018 [PubMed: 25881932]
17. Cheng S, Shah SH, Corwin EJ, Fiehn O, Fitzgerald RL, Gerszten RE, Illig T, Rhee EP, Srinivas PR, Wang TJ, Jain M (2017) Potential Impact and Study Considerations of Metabolomics in Cardiovascular Health and Disease: A Scientific Statement From the American Heart Association. Circ Cardiovasc Genet 10 doi:10.1161/hcg.0000000000000032

18. Damy T, Kirsch M, Khouzami L, Caramelle P, Le Corvoisier P, Roudot-Thoraval F, Dubois-Rande JL, Hittinger L, Pavoine C, Pecker F (2009) Glutathione deficiency in cardiac patients is related to the functional status and structural cardiac abnormalities. PLoS One 4:e4871doi:10.1371/journal.pone.0004871 [PubMed: 19319187]
19. Deidda M, Piras C, Dessalvi CC, Locci E, Barberini L, Torri F, Ascedu F, Atzori L, Mercuro G (2015) Metabolomic approach to profile functional and metabolic changes in heart failure. J Transl Med 13:297doi:10.1186/s12967-015-0661-3 [PubMed: 26364058]
20. Diakos NA, Navankasattusas S, Abel ED, Rutter J, McCreath L, Ferrin P, McKellar SH, Miller DV, Park SY, Richardson RS, Deberardinis R, Cox JE, Kfoury AG, Selzman CH, Stehlik J, Fang JC, Li DY, Drakos SG (2016) Evidence of Glycolysis Up-Regulation and Pyruvate Mitochondrial Oxidation Mismatch During Mechanical Unloading of the Failing Human Heart: Implications for Cardiac Reloading and Conditioning. JACC Basic Transl Sci 1:432–444 doi:10.1016/j.jacbts.2016.06.009 [PubMed: 28497127]
21. Du Z, Shen A, Huang Y, Su L, Lai W, Wang P, Xie Z, Xie Z, Zeng Q, Ren H, Xu D (2014) 1H-NMR-based metabolic analysis of human serum reveals novel markers of myocardial energy expenditure in heart failure patients. PLoS One 9:e88102doi:10.1371/journal.pone.0088102 [PubMed: 24505394]
22. Fiehn O (2016) Metabolomics by Gas Chromatography-Mass Spectrometry: Combined Targeted and Untargeted Profiling. Curr Protoc Mol Biol 114:30.34.31–30.34.32 doi:10.1002/0471142727.mb3004s114 [PubMed: 27038389]
23. Funaya H, Kitakaze M, Node K, Minamino T, Komamura K, Hori M (1997) Plasma adenosine levels increase in patients with chronic heart failure. Circulation 95:1363–1365, [PubMed: 9118500]
24. Gan XT, Ettinger G, Huang CX, Burton JP, Haist JV, Rajapurohitam V, Sidaway JE, Martin G, Gloor GB, Swann JR, Reid G, Karmazyn M (2014) Probiotic administration attenuates myocardial hypertrophy and heart failure after myocardial infarction in the rat. Circ Heart Fail 7:491–499 doi:10.1161/circheartfailure.113.000978 [PubMed: 24625365]
25. Gerber Y, Weston SA, Enriquez-Sarano M, Manemann SM, Chamberlain AM, Jiang R, Roger VL (2016) Atherosclerotic Burden and Heart Failure After Myocardial Infarction. JAMA Cardiol 1:156–162 doi:10.1001/jamacardio.2016.0074 [PubMed: 27437886]
26. Giannecchini M, Matteucci M, Pesi R, Sgarrella F, Tozzi MG, Camici M (2005) Uptake and utilization of nucleosides for energy repletion. Int J Biochem Cell Biol 37:797–808 doi:10.1016/j.biocel.2004.10.005 [PubMed: 15694839]
27. Gourine AV, Hu Q, Sander PR, Kuzmin AI, Hanafy N, Davydova SA, Zaretsky DV, Zhang J (2004) Interstitial purine metabolites in hearts with LV remodeling. Am J Physiol Heart Circ Physiol 286:H677–684 doi:10.1152/ajpheart.00305.2003 [PubMed: 14563662]
28. Gupte AA, Hamilton DJ, Cordero-Reyes AM, Youker KA, Yin Z, Estep JD, Stevens RD, Wenner B, Ilkayeva O, Loebe M, Peterson LE, Lyon CJ, Wong ST, Newgard CB, Torre-Amione G, Taegtmeyer H, Hsueh WA (2014) Mechanical unloading promotes myocardial energy recovery in human heart failure. Circ Cardiovasc Genet 7:266–276 doi:10.1161/circgenetics.113.000404 [PubMed: 24825877]
29. Hafstad AD, Nabeebaccus AA, Shah AM (2013) Novel aspects of ROS signalling in heart failure. Basic Res Cardiol 108:359doi:10.1007/s00395-013-0359-8 [PubMed: 23740217]
30. Hasko G, Kuhel DG, Nemeth ZH, Mabley JG, Stachlewitz RF, Virag L, Lohinai Z, Southan GJ, Salzman AL, Szabo C (2000) Inosine inhibits inflammatory cytokine production by a posttranscriptional mechanism and protects against endotoxin-induced shock. J Immunol 164:1013–1019, [PubMed: 10623851]
31. Heusch P, Canton M, Aker S, van de Sand A, Konietzka I, Rassaf T, Menazza S, Brodde OE, Di Lisa F, Heusch G, Schulz R (2010) The contribution of reactive oxygen species and p38 mitogen-activated protein kinase to myofilament oxidation and progression of heart failure in rabbits. Br J Pharmacol 160:1408–1416 doi:10.1111/j.1476-5381.2010.00793.x [PubMed: 20590631]
32. Hunter WG, Kelly JP, McGarrah RW 3rd, Kraus WE, Shah SH (2016) Metabolic Dysfunction in Heart Failure: Diagnostic, Prognostic, and Pathophysiologic Insights From Metabolomic Profiling. Curr Heart Fail Rep 13:119–131 doi:10.1007/s11897-016-0289-5 [PubMed: 27216948]

33. Huxtable R, Bressler R (1974) Taurine concentrations in congestive heart failure. Science 184:1187–1188, [PubMed: 4833255]
34. Ito T, Muraoka S, Takahashi K, Fujio Y, Schaffer SW, Azuma J (2009) Beneficial effect of taurine treatment against doxorubicin-induced cardiotoxicity in mice. Adv Exp Med Biol 643:65–74 doi: 10.1007/978-0-387-75681-3_7 [PubMed: 19239137]
35. Ito T, Yoshikawa N, Schaffer SW, Azuma J (2014) Tissue taurine depletion alters metabolic response to exercise and reduces running capacity in mice. J Amino Acids 2014:964680doi: 10.1155/2014/964680 [PubMed: 25478210]
36. Jong CJ, Azuma J, Schaffer S (2012) Mechanism underlying the antioxidant activity of taurine: prevention of mitochondrial oxidant production. Amino Acids 42:2223–2232 doi:10.1007/s00726-011-0962-7 [PubMed: 21691752]
37. Jong CJ, Ito T, Mozaffari M, Azuma J, Schaffer S (2010) Effect of beta-alanine treatment on mitochondrial taurine level and 5-taurinomethyluridine content. J Biomed Sci 17 Suppl 1:S25doi: 10.1186/1423-0127-17-s1-s25 [PubMed: 20804600]
38. Jong CJ, Ito T, Prentice H, Wu JY, Schaffer SW (2017) Role of Mitochondria and Endoplasmic Reticulum in Taurine-Deficiency-Mediated Apoptosis. Nutrients 9 doi:10.3390/nu9080795
39. Jong CJ, Ito T, Schaffer SW (2015) The ubiquitin-proteasome system and autophagy are defective in the taurine-deficient heart. Amino Acids 47:2609–2622 doi:10.1007/s00726-015-2053-7 [PubMed: 26193770]
40. Kang SM, Park JC, Shin MJ, Lee H, Oh J, Ryu DH, Hwang GS, Chung JH (2011) (1)H nuclear magnetic resonance based metabolic urinary profiling of patients with ischemic heart failure. Clin Biochem 44:293–299 doi:10.1016/j.clinbiochem.2010.11.010 [PubMed: 21167146]
41. Kapoor JR, Kapoor R, Ju C, Heidenreich PA, Eapen ZJ, Hernandez AF, Butler J, Yancy CW, Fonarow GC (2016) Precipitating Clinical Factors, Heart Failure Characterization, and Outcomes in Patients Hospitalized With Heart Failure With Reduced, Borderline, and Preserved Ejection Fraction. JACC Heart Fail 4:464–472 doi:10.1016/j.jchf.2016.02.017 [PubMed: 27256749]
42. Kato T, Niizuma S, Inuzuka Y, Kawashima T, Okuda J, Tamaki Y, Iwanaga Y, Narazaki M, Matsuda T, Soga T, Kita T, Kimura T, Shioi T (2010) Analysis of metabolic remodeling in compensated left ventricular hypertrophy and heart failure. Circ Heart Fail 3:420–430 doi:10.1161/circheartfailure.109.888479 [PubMed: 20176713]
43. Lai L, Leone TC, Keller MP, Martin OJ, Broman AT, Nigro J, Kapoor K, Koves TR, Stevens R, Ilkayeva OR, Vega RB, Attie AD, Muoio DM, Kelly DP (2014) Energy metabolic reprogramming in the hypertrophied and early stage failing heart: a multisystems approach. Circ Heart Fail 7:1022–1031 doi:10.1161/circheartfailure.114.001469 [PubMed: 25236884]
44. Lewis CW, Atkins BZ, Hutcheson KA, Gillen CT, Reedy MC, Glower DD, Taylor DA (1998) A load-independent in vivo model for evaluating therapeutic interventions in injured myocardium. Am J Physiol 275:H1834–1844, [PubMed: 9815092]
45. Linster CL, Van Schaftingen E (2007) Vitamin C. Biosynthesis, recycling and degradation in mammals. Febs j 274:1–22 doi:10.1111/j.1742-4658.2006.05607.x
46. Lopaschuk GD (2017) Metabolic Modulators in Heart Disease: Past, Present, and Future. Can J Cardiol 33:838–849 doi:10.1016/j.cjca.2016.12.013 [PubMed: 28279520]
47. Maekawa K, Hirayama A, Iwata Y, Tajima Y, Nishimaki-Mogami T, Sugawara S, Ueno N, Abe H, Ishikawa M, Murayama M, Matsuzawa Y, Nakanishi H, Ikeda K, Arita M, Taguchi R, Minamino N, Wakabayashi S, Soga T, Saito Y (2013) Global metabolomic analysis of heart tissue in a hamster model for dilated cardiomyopathy. J Mol Cell Cardiol 59:76–85 doi:10.1016/j.yjmcc.2013.02.008 [PubMed: 23454301]
48. McGarrah RW, Crown SB, Zhang GF, Shah SH, Newgard CB (2018) Cardiovascular Metabolomics. Circ Res 122:1238–1258 doi:10.1161/circresaha.117.311002 [PubMed: 29700070]
49. Mueller-Hennessen M, Dungen HD, Lutz M, Trippel TD, Kreuter M, Sigl J, Muller OJ, Tahirovic E, Witt H, Ternes P, Carvalho S, Peter E, Rein D, Schatz P, Herth F, Giannitsis E, Weis T, Frey N, Katus HA (2017) A Novel Lipid Biomarker Panel for the Detection of Heart Failure with Reduced Ejection Fraction. Clin Chem 63:267–277 doi:10.1373/clinchem.2016.257279 [PubMed: 28062623]

50. Newman WH, Frangakis CJ, Grosso DS, Bressler R (1977) A relation between myocardial taurine contest and pulmonary wedge pressure in dogs with heart failure. Physiol Chem Phys 9:259–263, [PubMed: 594193]
51. Nickel A, Loffler J, Maack C (2013) Myocardial energetics in heart failure. Basic Res Cardiol 108:358doi:10.1007/s00395-013-0358-9 [PubMed: 23740216]
52. Overmyer KA, Thonusin C, Qi NR, Burant CF, Evans CR (2015) Impact of anesthesia and euthanasia on metabolomics of mammalian tissues: studies in a C57BL/6J mouse model. PLoS One 10:e0117232doi:10.1371/journal.pone.0117232 [PubMed: 25658945]
53. Peterson MB, Mead RJ, Welty JD (1973) Free amino acids in congestive heart failure. J Mol Cell Cardiol 5:139–147, [PubMed: 4704669]
54. Ramila KC, Jong CJ, Pastukh V, Ito T, Azuma J, Schaffer SW (2015) Role of protein phosphorylation in excitation-contraction coupling in taurine deficient hearts. Am J Physiol Heart Circ Physiol 308:H232–239 doi:10.1152/ajpheart.00497.2014 [PubMed: 25437920]
55. Ruiz M, Labarthe F, Fortier A, Bouchard B, Thompson Legault J, Bolduc V, Rigal O, Chen J, Ducharme A, Crawford PA, Tardif JC, Des Rosiers C (2017) Circulating acylcarnitine profile in human heart failure: a surrogate of fatty acid metabolic dysregulation in mitochondria and beyond. Am J Physiol Heart Circ Physiol 313:H768–h781 doi:10.1152/ajpheart.00820.2016 [PubMed: 28710072]
56. Schaffer S, Kim HW (2018) Effects and Mechanisms of Taurine as a Therapeutic Agent. Biomol Ther (Seoul) 26:225–241 doi:10.4062/biomolther.2017.251 [PubMed: 29631391]
57. Schaffer SW, Azuma J, Madura JD (1995) Mechanisms underlying taurine-mediated alterations in membrane function. Amino Acids 8:231–246 doi:10.1007/bf00806821 [PubMed: 24186401]
58. Schaffer SW, Jong CJ, Ramila KC, Azuma J (2010) Physiological roles of taurine in heart and muscle. J Biomed Sci 17 Suppl 1:S2doi:10.1186/1423-0127-17-s1-s2 [PubMed: 20804594]
59. Schaffer SW, Shimada-Takaura K, Jong CJ, Ito T, Takahashi K (2016) Impaired energy metabolism of the taurinedeficient heart. Amino Acids 48:549–558 doi:10.1007/s00726-015-2110-2 [PubMed: 26475290]
60. Schulz TJ, Westermann D, Isken F, Voigt A, Laube B, Thierbach R, Kuhlow D, Zarse K, Schomburg L, Pfeiffer AF, Tschope C, Ristow M (2010) Activation of mitochondrial energy metabolism protects against cardiac failure. Aging (Albany NY) 2:843–853 doi:10.18632/aging.100234 [PubMed: 21084725]
61. Shafy A, Molinie V, Cortes-Morichetti M, Hupertan V, Lila N, Chachques JC (2012) Comparison of the effects of adenosine, inosine, and their combination as an adjunct to reperfusion in the treatment of acute myocardial infarction. ISRN Cardiol 2012:326809doi:10.5402/2012/326809 [PubMed: 22462024]
62. Shah SH, Hunter WG (2017) Realizing the Potential of Metabolomics in Heart Failure: Signposts on the Path to Clinical Utility. JACC Heart Fail 5:833–836 doi:10.1016/j.jchf.2017.08.025 [PubMed: 29096793]
63. Shah SH, Kraus WE, Newgard CB (2012) Metabolomic profiling for the identification of novel biomarkers and mechanisms related to common cardiovascular diseases: form and function. Circulation 126:1110–1120 doi:10.1161/circulationaha.111.060368 [PubMed: 22927473]
64. Sheeran FL, Pepe S (2016) Posttranslational modifications and dysfunction of mitochondrial enzymes in human heart failure. Am J Physiol Endocrinol Metab 311:E449–460 doi:10.1152/ajpendo.00127.2016 [PubMed: 27406740]
65. Shen W, Asai K, Uechi M, Mathier MA, Shannon RP, Vatner SF, Ingwall JS (1999) Progressive loss of myocardial ATP due to a loss of total purines during the development of heart failure in dogs: a compensatory role for the parallel loss of creatine. Circulation 100:2113–2118, [PubMed: 10562269]
66. Shimura D, Nakai G, Jiao Q, Osanai K, Kashikura K, Endo K, Soga T, Goda N, Minamisawa S (2013) Metabolomic profiling analysis reveals chamber-dependent metabolite patterns in the mouse heart. Am J Physiol Heart Circ Physiol 305:H494–505 doi:10.1152/ajpheart.00867.2012 [PubMed: 23792677]

67. Siddiqi N, Singh S, Beadle R, Dawson D, Frenneaux M (2013) Cardiac metabolism in hypertrophy and heart failure: implications for therapy. Heart Fail Rev 18:595–606 doi:10.1007/s10741-012-9359-2 [PubMed: 23124940]
68. Skogerson K, Wohlgemuth G, Barupal DK, Fiehn O (2011) The volatile compound BinBase mass spectral database. BMC Bioinformatics 12:321doi:10.1186/1471-2105-12-321 [PubMed: 21816034]
69. Smiseth OA, Gunnes P, Sand T, Mjos OD (1989) Inosine causing insulin release and increased myocardial uptake of carbohydrates relative to free fatty acids in dogs. Clin Physiol 9:27–38, [PubMed: 2650958]
70. Sun H, Olson KC, Gao C, Prosdocimo DA, Zhou M, Wang Z, Jeyaraj D, Youn JY, Ren S, Liu Y, Rau CD, Shah S, Ilkayeva O, Gui WJ, William NS, Wynn RM, Newgard CB, Cai H, Xiao X, Chuang DT, Schulze PC, Lynch C, Jain MK, Wang Y (2016) Catabolic Defect of Branched-Chain Amino Acids Promotes Heart Failure. Circulation 133:2038–2049 doi:10.1161/circulationaha.115.020226 [PubMed: 27059949]
71. Takihara K, Azuma J, Awata N, Ohta H, Hamaguchi T, Sawamura A, Tanaka Y, Kishimoto S, Sperelakis N (1986) Beneficial effect of taurine in rabbits with chronic congestive heart failure. Am Heart J 112:1278–1284, [PubMed: 3788775]
72. Teichholz LE, Kreulen T, Herman MV, Gorlin R (1976) Problems in echocardiographic volume determinations: echocardiographic-angiographic correlations in the presence of absence of asynergy. Am J Cardiol 37:7–11, [PubMed: 1244736]
73. Tenori L, Hu X, Pantaleo P, Alterini B, Castelli G, Olivotto I, Bertini I, Luchinat C, Gensini GF (2013) Metabolomic fingerprint of heart failure in humans: a nuclear magnetic resonance spectroscopy analysis. Int J Cardiol 168:e113–115 doi:10.1016/j.ijcard.2013.08.042 [PubMed: 24007967]
74. Turer AT (2013) Using metabolomics to assess myocardial metabolism and energetics in heart failure. J Mol Cell Cardiol 55:12–18 doi:10.1016/j.yjmcc.2012.08.025 [PubMed: 22982115]
75. Wang J, Li Z, Chen J, Zhao H, Luo L, Chen C, Xu X, Zhang W, Gao K, Li B, Zhang J, Wang W (2013) Metabolomic identification of diagnostic plasma biomarkers in humans with chronic heart failure. Mol Biosyst 9:2618–2626 doi:10.1039/c3mb70227h [PubMed: 23959290]
76. Wang W, Zhang F, Xia Y, Zhao S, Yan W, Wang H, Lee Y, Li C, Zhang L, Lian K, Gao E, Cheng H, Tao L (2016) Defective branched chain amino acid catabolism contributes to cardiac dysfunction and remodeling following myocardial infarction. Am J Physiol Heart Circ Physiol 311:H1160–h1169 doi:10.1152/ajpheart.00114.2016 [PubMed: 27542406]
77. Wang YT, Popovic ZB, Efimov IR, Cheng Y (2012) Longitudinal study of cardiac remodelling in rabbits following infarction. Can J Cardiol 28:230–238 doi:10.1016/j.cjca.2011.11.003 [PubMed: 22265993]
78. Wende AR, Brahma MK, McGinnis GR, Young ME (2017) Metabolic Origins of Heart Failure. JACC Basic Transl Sci 2:297–310 doi:10.1016/j.jacbts.2016.11.009 [PubMed: 28944310]
79. Yancy CW, Jessup M, Bozkurt B, Butler J, Casey DE Jr., Drazner MH, Fonarow GC, Geraci SA, Horwich T, Januzzi JL, Johnson MR, Kasper EK, Levy WC, Masoudi FA, McBride PE, McMurray JJ, Mitchell JE, Peterson PN, Riegel B, Sam F, Stevenson LW, Tang WH, Tsai EJ, Wilkoff BL (2013) 2013 ACCF/AHA guideline for the management of heart failure: a report of the American College of Cardiology Foundation/American Heart Association Task Force on practice guidelines. Circulation 128:e240–327 doi:10.1161/CIR.0b013e31829e8776 [PubMed: 23741058]
80. Zordoky BN, Sung MM, Ezekowitz J, Mandal R, Han B, Bjorndahl TC, Bouatra S, Anderson T, Oudit GY, Wishart DS, Dyck JR (2015) Metabolomic fingerprint of heart failure with preserved ejection fraction. PLoS One 10:e0124844doi:10.1371/journal.pone.0124844 [PubMed: 26010610]

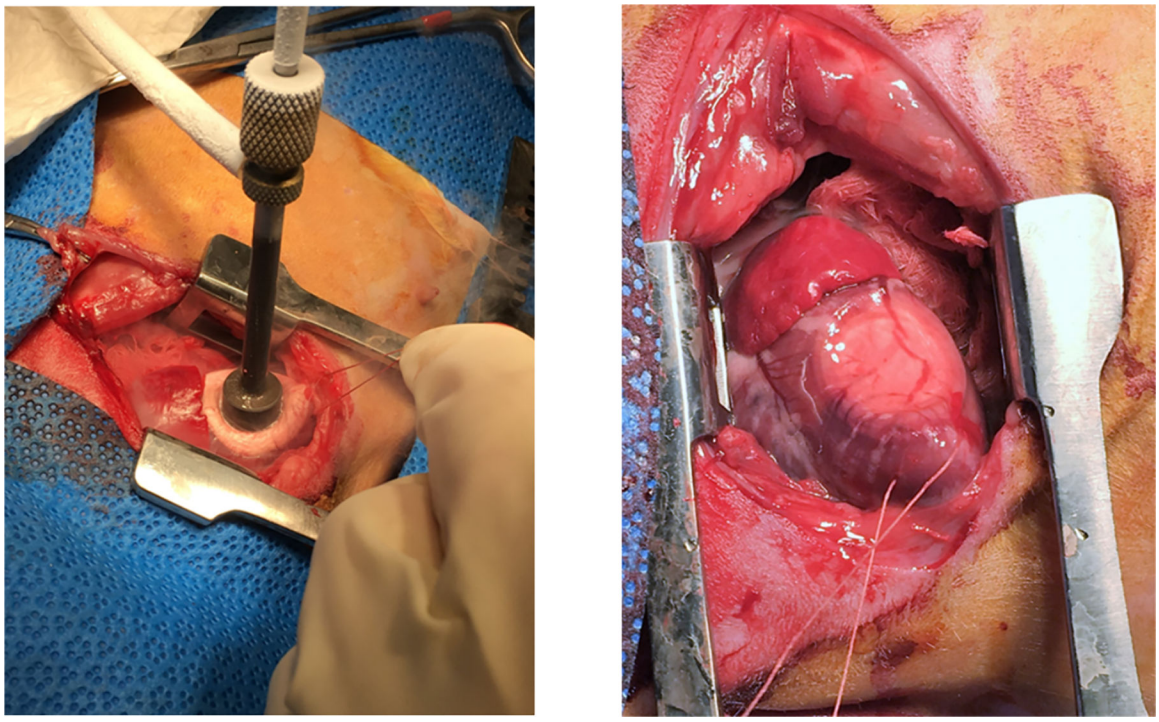

Fig. 1.
Cryo-probe freezing the myocardium and the effected region immediately post the 3-minute freeze.

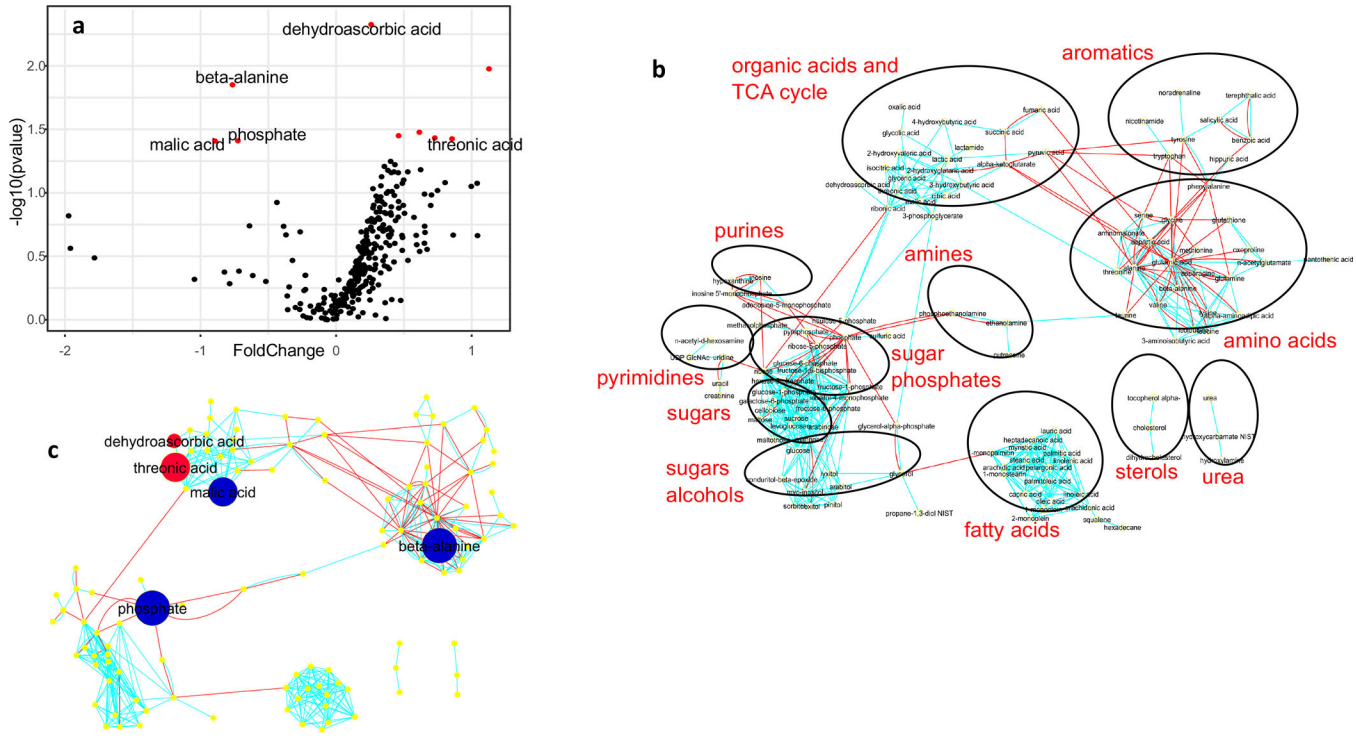

Fig. 2.

Volcano plot (a) of serum metabolites wherein red dots indicate significantly different signals between MI and Sham rabbits. ($p<.05$: log transformed data); Network regions (b) and metabolite comparisons within the regions for serum. Red dot indicates that the compound signal for MI rabbits was greater than Sham rabbits while blue dot indicates that the signal for MI rabbits was less than Sham rabbits ($p < .05$, log data analysis). Size of the dot indicates the relative difference.

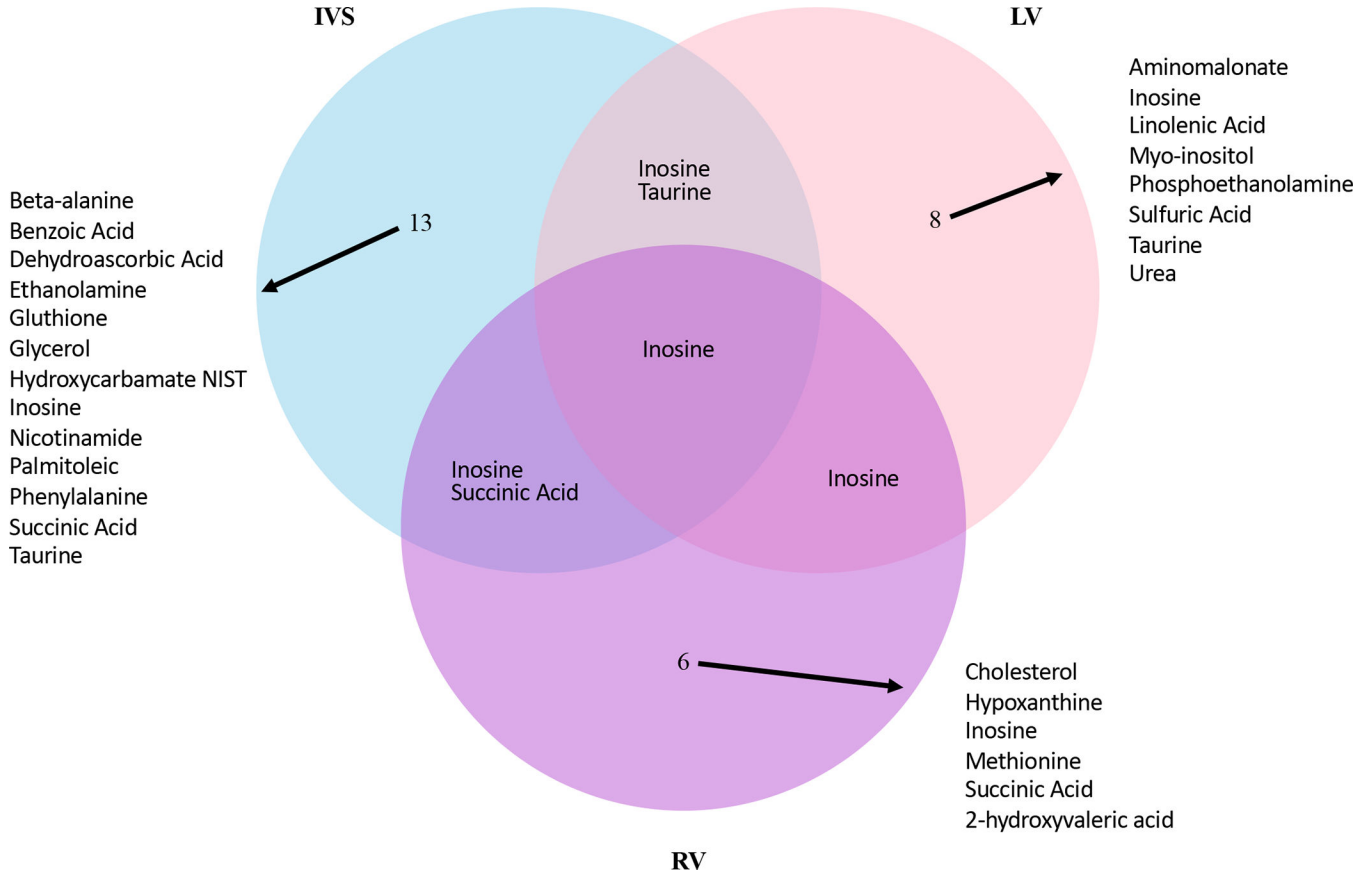

Fig. 3.

Venn Diagram of compound signals present in the Interventricular Septum (IVS), Left Ventricle (LV) and Right Ventricle (RV) that were significantly different between Mi and Sham rabbits. Log transformed data analysis.

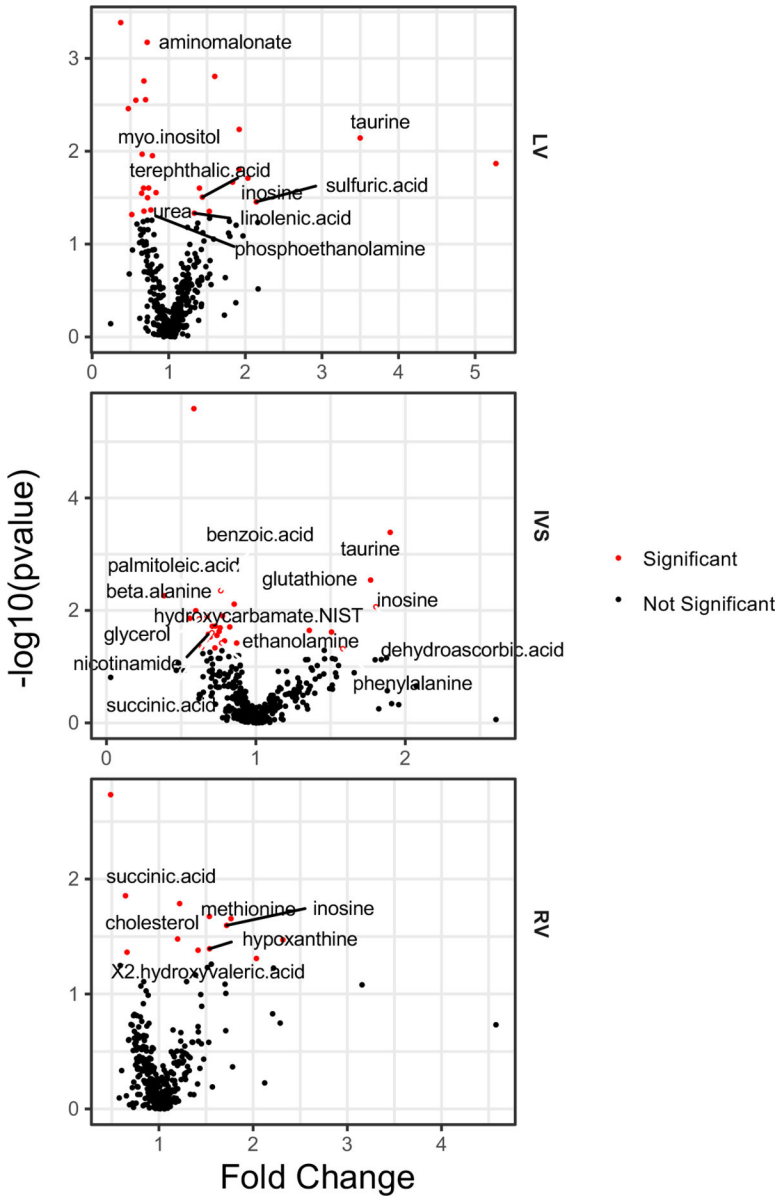

Fig. 4.

Volcano plots of compounds present in the Left Ventricle (LV), Intraventricular Septum (IVS) and Right Ventricle (RV) of myocardial infarction (MI) and sham rabbits. Red dots indicate that compound levels are significantly different between MI and Sham rabbits (p< . 05; log data analysis).

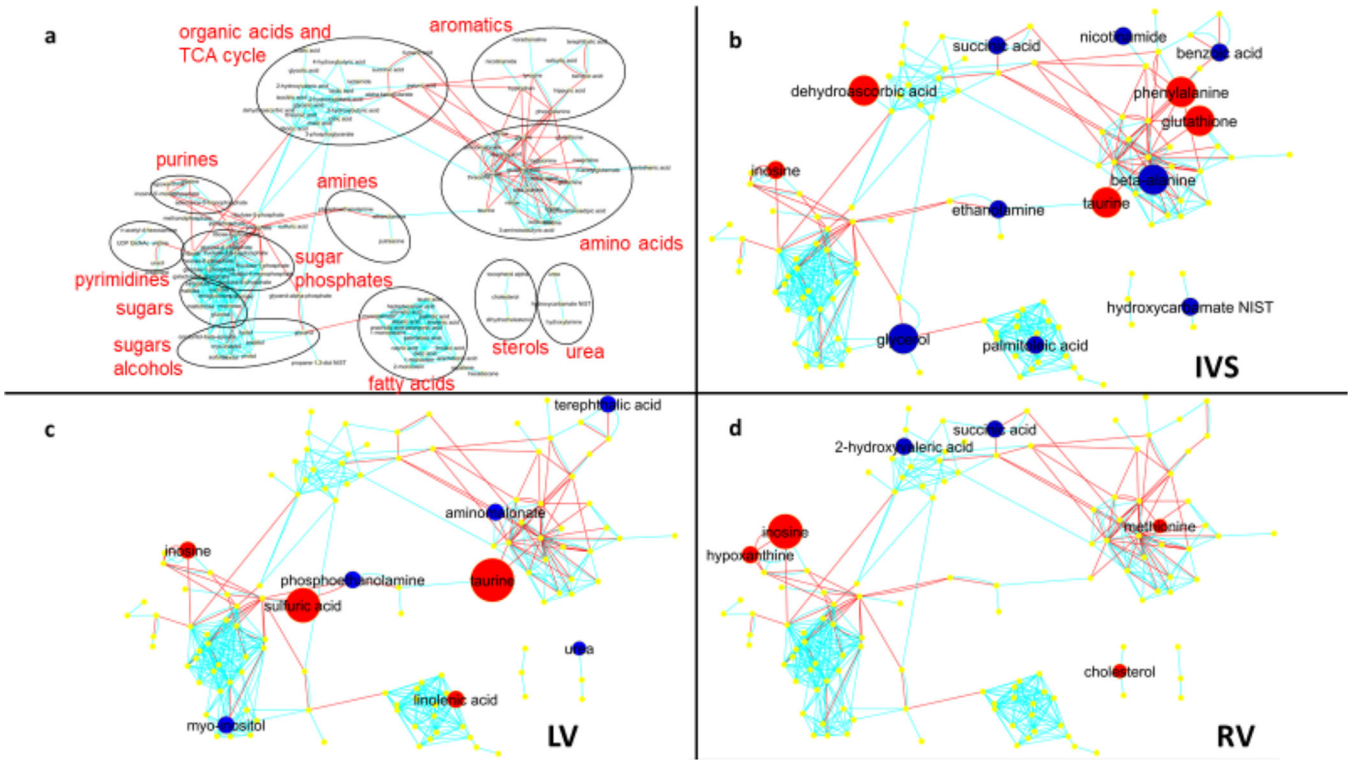

Fig. 5.

Network regions (a) and compound comparisons for the three myocardial regions: (b) Interventricular Septum - IVS, (c) Left Ventricle – LV, (d) Right Ventricle – RV. Red dot indicates that the compound signal for MI rabbits was greater than Sham rabbits while blue dot indicates that the signal for MI rabbits was less than Sham rabbits ($p < .05$, log data analysis). Size of the dot indicates the relative difference.

Table 1

Heart and Body weights of MI and Sham Rabbits.[a]

Variable[b]	Shams (n = 6)	MI (n= 10)	p value[c]
Body Wt (Kg)	4.72 ± 0.06	4.42 ± 0.10	0.06
Heart Wt (gms)	10.32 ± 0.25	12.65 ± 0.80	0.047
HT/BW	2.22 ± 0.04	2.85 ± 0.16	0.017
HT/TL	0.092 ± .002	0.116 ± 0.007	0.02
LV Wt (gms)	6.19 ± 0.19	6.59 ± 0.36	0.43
LV/BW	1.31 ± 0.04	1.48 ± 0.06	0.05
LV/TL	0.055 ± 0.001	0.059 ± 0.003	0.34
RV Wt (gms)	1.96 ± 0.07	2.68 ± 0.26	0.05
RV/BW	0.42 ± 0.02	0.60 ± 0.05	0.02
RV/TL	0.017 + 0.001	0.024 + 0.002	0.05

[a] Data presented as Mean ± SEM for Sham-operated and Myocardial Infarction (MI) Rabbits.

[b] LV = left ventricle; RV = right ventricle; TL = Tibial Length; HT = heart; BW = body weight;

[c] p values represent an unpaired t-test comparing Sham and MI rabbits. Graph Pad/Prism 6 Statistical Software.

Table 2

Echocardiographic Responses to a Cryo-Myocardial Infarction.

Variable[a]	Group[b]		Pre[c]	4 Wks	8 Wks	12 Wks	ANOVA-RM[d]
HR (bpm)	MI Sham		220 ± 7 219 ± 7	245 ± 8 221 ± 7	225 ± 11 222 ± 9	226 ± 9 213 ± 13	0.66
EDD (mm)	MI Sham		16.7 ± 0.2 17.0 ± 0.3	21.1 ± 0.6* 17.3 + 07	23.0 ± 0.8* 17.2 ± 0.7	23.3 ± 0.9* 17.3 ± 0.5	0.001
ESD (mm)	MI Sham		11.0 ± 0.2 11.2 ± 0.2	16.9 ± 0.5* 11.7 ± 0.7	18.5 ± 0.8* 11.8 ± 0.7	19.0 ± 0.7* 11.5 ± 0.6	0.001
IVSd (mm)	MI Sham		2.38 ± 0.07 2.54 ± 0.05	2.63 ± 0.10 2.67 ± 0.12	2.6 ± 0.10 2.97 ± 0.12	2.76 ± 0.14 2.64 ± 0.12	0.15
IVSs (mm)	MI Sham		3.61 ± 0.06 3.91 ± 0.09	3.80 ± 0.13 4.08 ± 0.20	3.61 ± 0.12* 4.46 ± 0.32	3.86 ± 0.19 3.89 ± 0.07	0.03
LVFWd (mm)	MI Sham		2.54 ± 0.07 2.68 ± 0.07	1.92 ± 0.12* 2.75 ± 0.14	1.88 ± 0.11* 3.05 ± 0.21	1.95 ± 0.14* 2.99 ± 0.22	0.03
LVFWs (mm)	MI Sham		4.03 ± 0.10 4.33 ± 0.13	2.50 ± 0.24* 4.31 ± 0.16	2.40 ± 0.21* 4.35 ± 0.28	2.23 ± 0.17* 4.07 ± 0.13	0.003
FS (%)	MI Sham		34.4 ± 0.8 34.2 ± 0.6	20.2 ± 0.8* 32.7 ± 1.8	18.7 ± 0.6* 31.7 ± 1.7	19.1 ± 0.7* 34.0 ± 1.4	0.001
Vcf (circ/s)	MI Sham		3.13 ± 0.09 2.99 ± 0.08	1.79 ± 0.07* 3.03 ± 0.15	1.74 ± 0.09* 2.95 ± 0.24	1.62 ± 0.04* 3.02 ± 0.17	0.001
EF (%)	MI Sham		63 ± 2 59 ± 1	38 ± 1* 57 ± 2	37 ± 2* 56 ± 2	35 ± 1* 59 ± 2	0.001

[a] HR= Heart rate, beats perm in.; EDD=End Diastolic Dimension; ESD= End Systolic Dimension; IVSd = Interventricular septum thickness in dsstole; IVSs= Interventricular septum thickness in systole; LVFWd = Left ventricular free wallthickness in dastole; LVFWs = Left ventricular free wall thickness h systole; FS = Fractional Shortening; Vcf = Circumferential fiber shortening; EF = Ejection Fraction.

[b] MI = Myocardial infarction group, n= 10; Sham = Sham operated group, n=6.

[c] Data presented as Mean ± SEM for pre-surgery (Pre) and 4, 8 and 12 weeks post-op;

[d] Analysis of Variance with repeated measures (ANOVA – RM) was used to compare the two groups overtime. Post-hoc comparisons were performed using Sidak's multiple comparison test.

* p< .001 vs Sham. Graph Pad/Prism 6 Statistical Software.

Table 3

Comparisons of Metabolites from Heart and Serum of MI and Sham MI Rabbits.[a]

		Source:	Left Ventricle Free Wall			Intraventricular Septum			Right Ventricle			Serum		
Network			**MI/Sham**	**Raw data**	**Log data**	**MI/Sham**	**Raw data**	**Log data**	**MI/Sham**	**Raw data**	**Log data**	**MI/Sham**	**Raw data**	**Log data**
Regions	**Metabolite**	**KEGG**	**Mean**	**p value**	**p value**	**Mean**	**p value**	**p value**	**Mean**	**p value**	**p value**	**Mean**	**p value**	**p value**
Amines	Ethanolamine	C00189				0.771	0.059	0.038						
	Phosphoethanolamine	C00346	0.767	0.083	0.043									
Amino Acids	Aspartic acid	C00049	1.875	0.046	0.070									
	Aminomalonate	C00872	0.719	0.001	0.001									
	Beta-alanine	C00099				0.557	0.013	0.014				0.589	0.023	0.014
	Glutathione	C00051				1.768	0.003	0.003						
	Methionine	C00073							1.220	0.012	0.016			
	Ta uri ne	C00245	3.499	0.001	0.007	1.899	0.001	0.000	3.156	0.036	0.083			
Aromatics	Benzoic Acid	C00180				0.765	0.009	0.004						
	Nicotinamide	C00153				0.682	0.004	0.027						
	Phenylalanine	C00079	1.445	0.047	0.075	1.582	0.040	0.048						
Fatty Acids	Linolenic acid	C06427	1.334	0.056	0.046									
	Palmitoleic	C08362				0.674	0.017	0.013						
	Stearic acid	C01530										1.262	0.048	0.075
Organic Acids	Dehydroascorbic acid	C05422				1.803	0.006	0.009				1.197	0.005	0.005
& TCA Cycle	Malic acid	C00711										0.539	0.060	0.039
	Succinic acid	C00042				0.706	0.049	0.025	0.645	0.026	0.014			
	Threonic acid	C01620							1.514	0.038	0.059	1.809	0.007	0.038
	2-hydroxyvaleric acid	na							0.662	0.040	0.043			
Phosphates	Phosphate	C00009										0.605	0.100	0.039
	Methanophosphate	na	1.970	0.017	0.082									
	Sulfuric acid(Sulfate)	C00059	2.143	0.020	0.035									
Purines	Hypoxanthine	C00262							1.537	0.041	0.040			
	Inosine	C00294	1.439	0.011	0.031	1.358	0.011	0.023	1.719	0.025	0.025			

		Source:	Left Ventricle Free Wall			Intraventricular Septum			Right Ventricle			Serum		
Network			**MI/Sham**	**Raw data**	**Log data**	**MI/Sham**	**Raw data**	**Log data**	**MI/Sham**	**Raw data**	**Log data**	**MI/Sham**	**Raw data**	**Log data**
Regions	**Metabolite**	**KEGG**	**Mean**	**p value**	**p value**	**Mean**	**p value**	**p value**	**Mean**	**p value**	**p value**	**Mean**	**p value**	**p value**
Sterols	Cholesterol	C00187							1.199	0.025	0.033			
Sugars	Conduritol-beta-epoxide	na				0.673	0.050	0.079						
Alcohol	Glycerol	C00116				0.621	0.020	0.014						
	Isothreitol	C16884										1.996	0.040	0.089
	Myo-inositol	C00137	0.787	0.012	0.011	0.870	0.078	0.064	0.864	0.127	0.094	1.541	0.056	0.066
Urea	Hydroxycarbamate NIST	na				0.761	0.024	0.020						
	Urea	C00086	0.835	0.032	0.028									

[a]KEGG = Compound identifier in the KEGG resource database; MI/Sham = ratio of the mean signal in MI and Sham rabbits; Raw data and Log2 data p values represent comparisons of MI and Sham rabbit signal values using Welch's t-test.